Journal of Power Sources 182 (2008) 377–382

Contents lists available at ScienceDirect

Journal of Power Sources

journal homepage: www.elsevier.com/locate/jpowsour

Short communication

Thermal behaviors of Ni-MH batteries using a novel impedance spectroscopy

Pu Xiao [a,b], Wenying Gao [c], Xinping Qiu [a,b,*], Wentao Zhu [a], Jie Sun [d], Liquan Chen [a,b]

[a] Key Laboratory of Organic Optoelectronics and Molecular Engineering, Department of Chemistry, Tsinghua University, Beijing 100084, China
[b] Laboratory of Advanced Power Sources, Graduate School at Shenzhen, Tsinghua University, Shenzhen 518055, China
[c] Key Lab of Bioorganic Phosphorous Chemistry and Chemical Biology, Department of Chemistry, Tsinghua University, Beijing 100084, China
[d] Institute of Chemical Defense, Beijing 102205, China

ARTICLE INFO

Article history:
Received 11 December 2007
Received in revised form 11 March 2008
Accepted 22 March 2008
Available online 29 March 2008

Keywords:
Heat generation
Ni-MH batteries
Novel impedance spectrum
Thermal behavior

ABSTRACT

In this paper, a novel impedance spectroscopy was used to describe the thermal behaviors of Ni-MH batteries. The impedance functions were derived similarly to electric impedance functions. The square of current was treated as a current equivalent and heat-flow as a voltage equivalent. The impedance spectra of batteries during charge showed that the combination of hydrogen and oxygen increased rapidly when charge rate was higher than 0.5 C. Thermal runaway might happen when battery was charged at temperature above 348 K even at a low charge rate. The cycling test showed that the charge efficiency of battery was the highest after cycling at high-rate for 10–100 cycles and decreased after more cycles. Different batteries showed different thermal behaviors which may be caused by the different structures of batteries.

© 2008 Published by Elsevier B.V.

1. Introduction

The temperature of Ni-MH battery increases when it is charged or discharged. For large Ni-MH batteries or battery packs, the heat generated from over potential and side-reaction may cause the battery overcharge and over discharge in the high-temperature region [1]. Therefore it is very important to study thermal behaviors of Ni-MH batteries. In situ studies of charge and discharge of batteries using electrochemical–calorimetric measurements have been reported in recent years [2–11]. Thermocouples have been used instead of calorimeters in some experiments to simplify the instruments [1,12–16]. However, the thermal analyses of these studies have been focused on heat response in the time-domain only. Barsoukov et al. [17] provided us a method to obtain a novel impedance spectrum of the response to arbitrary excitation and they obtained the thermal impedance spectra for Li-ion batteries using heat pulse as excitation [18]. The impedance spectrum in frequency-domain relating with the excitation signal and response signal may offer more information of batteries.

In this study, a novel impedance spectrum was obtained by using the charge current as excitation and the heat generation as response. An equivalent circuit was used to describe battery reaction which caused heat generation during charge. The values of the resistance and the capacitance were obtained by fitting the impedance spectrum.

2. Derivation of the novel impedance functions

The impedance spectrum of an electrical device is usually obtained by applying an excitation signal, and analyzing the response signal [19]. The novel impedance functions can be derived similarly to electric impedance functions. The square of current is treated as a current equivalent and heat-flow as a voltage equivalent [18]. The novel impedance function can be obtained by the following equation:

$$Z(s) = \frac{L\{H(t)\}}{L\{i^2(t)\}} \tag{1}$$

where $L\{\}$ denotes a Laplace transform, $H(t)$ is a heat-flow response function, and $i^2(t)$ is an excitation current function in the time-domain. For constant current charge process, $i^2(t)$ can be expressed as the square of applied current multiplied by Heavisde step-function $\Phi(t)$. $\Phi(t)$ is defined as 0 if $t < 0$ and 1 otherwise:

$$i^2(t) = I^2\Phi(t) \tag{2}$$

Its Laplace transform can be described in the following equation:

$$L\{i^2(t)\} = \frac{I^2}{s} \tag{3}$$

* Corresponding author at: Key Laboratory of Organic Optoelectronics and Molecular Engineering, Department of Chemistry, Tsinghua University, Beijing 100084, China. Tel.: +86 10 62794234; fax: +86 10 62794234.
E-mail address: qiuxp@mail.tsinghua.edu.cn (X. Qiu).

0378-7753/$ – see front matter © 2008 Published by Elsevier B.V.
doi:10.1016/j.jpowsour.2008.03.055

A set of time-dependent samples H_i collected with time interval δt during sampling period Δt are obtained from an experiment. The direct way to obtain the impedance function using numerical integration are very sensitive to noise, so a carrier function Laplace transform (CFLT) [17] which has superior noise-rejection capability is used here to calculate $L\{H(t)\}$. The carrier function has sufficient degrees of freedom to describe all possible system responses. The parameter obtained by fitting the experiment data to the carrier function can be substituted into an analytical expression of the Laplace transform of such a function. The sum of an adaptively chosen number of exponents is used as a carrier function to calculate $L\{H(t)\}$ [18]:

$$H(t) = \sum_{i=0}^{n} k_i \, e^{-(t/\tau_i)} \tag{4}$$

here k_i and τ_i are parameters that can be obtained by fitting the experiment data to the carrier function.

Laplace transform is as follows:

$$L\{H(t)\} = \sum_{i=0}^{n} \frac{k_i}{s + (1/\tau_i)} \tag{5}$$

Therefore, the impedance function using the square of current as excitation signal and heat-flow as response signal can be calculated from Eqs. (1), (3) and (5):

$$Z(s) = \left(\frac{s}{I^2}\right) \sum_{i=0}^{n} \frac{k_i}{s + (1/\tau_i)} \tag{6}$$

here I^2 is the square of the magnitude of the current applied to battery at time 0, and s is $2\pi fi$ where the boundaries of frequency range are given by Nyquist theorem, $f_{max} = 1/2\delta t$ and $f_{min} = 1/\Delta t$.

The heat generation of Ni-MH batteries during charge can be divided into two parts [1]:

(1) heat due to the main reactions, represented as $I(E - E_0 - T\Delta S/nF)(1 - \xi)$.
(2) heat due to the side-reactions, represented as $IE\xi$.

So the total heat generation of Ni-MH batteries during charge can be written as

$$H(t) = IE\xi + I\left(\frac{E - E_0 - T\Delta S}{nF}\right)(1 - \xi) \tag{7}$$

here ξ is the ratio of current for the combination of hydrogen and oxygen, E is the battery voltage during charge, I is the charge current, E_0 is the standard voltage of Ni-MH battery, T is the battery temperature, F is the number of Faraday, ΔS is the entropy change and n is the number of mole of electrons.

By simplifying Eq. (7), we get:

$$H(t) = I\left(\frac{E - E_0 - T\Delta S}{nF}\right) + I\xi\left(\frac{E_0 + T\Delta S}{nF}\right) \tag{8}$$

Since

$$E - E_0 = IR + \Delta\phi \tag{9}$$

So Eq. (8) can also be written as

$$H(t) = I\left(\frac{IR + \Delta\phi - T\Delta S}{nF}\right) + I\xi\left(\frac{E_0 + T\Delta S}{nF}\right) \tag{10}$$

here $\Delta\phi$ is the over potential, R is the sum of ohmic resistance. The temperature of battery during charge is stable when SOC (state of charge) is between 40% and 60%, and the heat absorbed by heat capacity of battery can be ignored. In this short period, according to the typical internal pressure curve and voltage curve of Ni-MH battery during charge [20], we can assume ξ and $\Delta\phi$ increase approximately linearly:

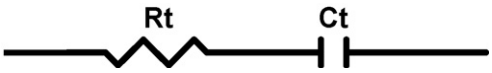

Fig. 1. Equivalent circuit corresponding to battery charged with constant current.

$$\xi = \xi_0 + k_\xi t \tag{11}$$

$$\Delta\phi = \Delta\phi_0 + k_{\Delta\phi} t \tag{12}$$

here ξ_0 is the initial value while k_ξ is the slope of the ratio of current for the combination reaction. And $\Delta\phi_0$ is the initial value while $k_{\Delta\phi}$ is the slope of the over potential and t is the sampling time. Applying Eqs. (11) and (12) to Eq. (10), we can get the following equation:

$$H(t) = I^2\left[R + \frac{\Delta\phi_0}{I} - \frac{T\Delta S}{nFI} + \xi_0\left(\frac{E_0 + T\Delta S/nF}{I}\right)\right] + I^2 t\left[k_\xi\left(\frac{E_0 + T\Delta S/nF}{I}\right) + \frac{k_{\Delta\phi}}{I}\right] \tag{13}$$

Eq. (13) can be divided into two parts: one part is independent of time that can be presented as I^2R_t; the other part increases with time that can be presented as I^2t/C_t.

So Eq. (13) can be written as

$$H(t) = I^2R_t + \frac{I^2 t}{C_t} \tag{14}$$

Higher the value of R_t, more the heat generation of battery, while the heat generation increases rapidly when the value of C_t is lower. So a higher value of R_t and a lower value of C_t indicate lower charge efficiency. According to Eqs. (13) and (14), the value of R_t is related to all the factors that cause heat generation, while the value of C_t is affected by the growth of over potential and combination of hydrogen and oxygen, so the value of C_t may have relationship with the porosity and the pore diameter of the electrode material.

The impedance equation of Eq. (14) obtained by Laplace transform is as follows:

$$Z(s) = R_t + \frac{1}{C_t s} \tag{15}$$

The equivalent circuit of Eq. (15) is a resistance in series with a capacitance as shown in Fig. 1.

3. Experimental

3.1. Samples

Cylindrical Ni-MH batteries of the R03 type manufactured by Energizer, GP and Uniross with different nominal capacities were bought from market (Fig. 2). The Ni-MH battery has the active material of NiOOH at the positive electrode and the active material of hydrogen as a metal hydride (MH) at the negative electrode, with OH^- transferring between the two electrodes as a charge or discharge reaction proceeds [1]. Detailed characteristics of the batteries are given in Table 1.

3.2. Apparatus

A twin-type differential heat conduction calorimeter (C80, Setaram), with the resolution of 10 μW, was used. A multi-channel battery testing system (BTS-5V/3A, Neware Tech. Limited) was used to charge and discharge the battery in the calorimeter and record the voltage and current. The battery testing system could measure voltage with accuracy of ±0.2% and current with accuracy of

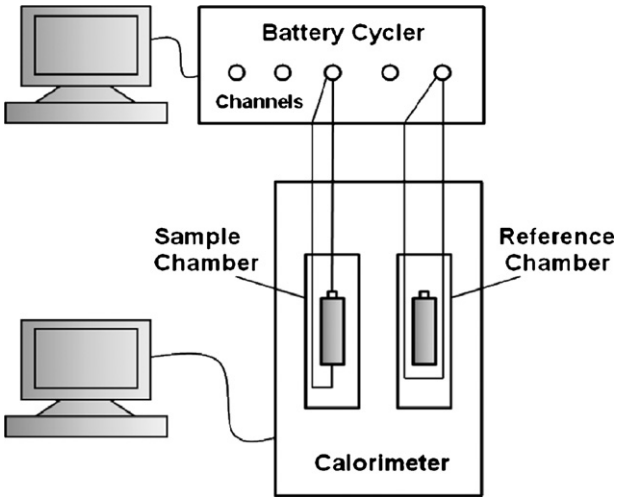

Fig. 2. Schematic diagram of the experimental setup.

±0.1%. As shown in Fig. 3, a battery of the same type was inserted into the reference chamber in the calorimeter to cancel the heat due to side-reaction except for the electrochemical side-reaction. Although the wires were not connected to the reference battery, they were also inserted into the reference chamber to balance the heat loss between sample and reference. The current that applied to wires in the sample chamber was the same as that applied to wires in the reference chamber, and the influence of heat generation by the resistance of the wires during charge could be ignored because the length of the wires in sample side was same as that in reference side [9].

Table 1
Characteristic parameters of batteries subjected to impedance measurement

Sample	Manufactures	Radius/height (mm)	Weight (g)	Nominal capacity (mAh)	Discharge capacity (mAh)
1	Energizer	10.5/44.5	12.18	850	797
2	GP	10.5/44.5	13.48	850	819
3	Uniross	10.5/44.5	11.42	700	677
4	GP	10.5/44.5	11.78	700	720

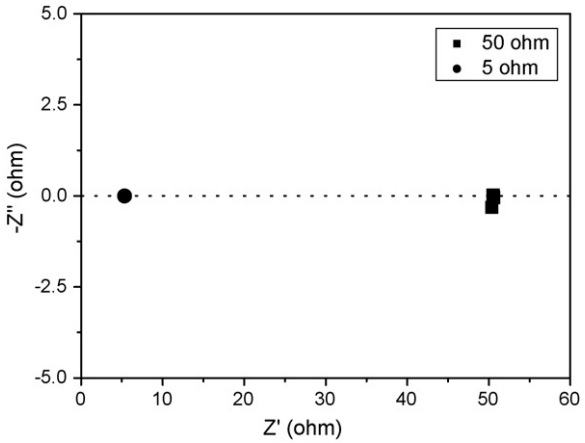

Fig. 3. Impedance spectra of a 50 Ω resistance and a 5 Ω resistance.

3.3. Experimental procedure

The charge and discharge current was determined from the charge and discharge rate with the discharge capacity. Samples were all charged until charged electricity reached 160% of the initial discharge capacity, then discharged at 0.2 C with the termination voltage of 1.0 V. The sampling period changed when battery was charged at different rates, so we adjusted the time interval to make the sum of sampling points are the same.

Constant current was applied to two resistors with different values, and the heat-flow of them was measured simultaneously. Heat-flow for sample 1 charged at different rates at 298 K was measured. Then heat-flow for sample 1 charged at 0.1 C at different temperatures was measured. Heat-flow for sample 2 charged at 0.3 C at 298 K after cycling different times at high-rate was measured. The charge and discharge rate was 2 C in the cycling. We also measured heat-flow for sample batteries from different manufactures with different discharge capacities when they were charged at 0.3 C at 298 K. A four order exponential decay function was used to describe the heat-flow curve as described in Eq. (4). The Laplace transforms of the heat-flow curve function and the constant current function can be obtained from Eqs. (5), (2) and (3). Therefore, we got the impedance spectra from Eq. (6).

4. Results and discussion

4.1. Impedance spectra of resistors generating heat

Constant current was applied to a 5 Ω resistor and a 50 Ω resistor, and the heat-flow of them was measured simultaneously. The impedance spectra of the two resistors were obtained using Eq. (6) as shown in Fig. 3. It can be seen that two points are on the real axis as expected. The equivalent circuit of a resistor using heat-flow as response signal and constant current as excitation signal is a resistance. The typical impedance spectrum of a resistance is a point on the real axis, and the values of resistances obtained directly are the same with the two values of resistances obtained from impedance, so the novel impedance functions are correct. As a result of the testing error, the spectrum of 50 Ω resistance does not concentrate well on the real axis.

4.2. Thermal behavior of Ni-MH battery charged at different rates

Fig. 4 shows the typical heat generation and voltage curves of sample 1 charged at 0.1, 0.2, 0.3, 0.4, 0.5, and 0.6 C, respectively. The temperature in the calorimeter was controlled to be 298 K during the test. It can be seen that heat generation and voltage increased with charge rate. Furthermore, heat generation can be divided into three parts. At the beginning of charge, heat generation is caused by the active material converting into a chargeable form. At the middle of charge, the discharged active material converting into the charged state gives out heat. At the end of charge, the combination of hydrogen and oxygen causes the temperature to rise [21]. Thus, the heat generation is stable and related to the main exothermic reactions at the middle of charge, so we chose the heat generation of SOC between 40% and 60% to obtain the impedance spectra as shown in Fig. 5. It can be seen that lines perpendicular to the real axis in the fourth quadrant which indicates a typical impedance spectrum of a resistance in series with a capacitance. Fig. 5 shows a good fit of the calculated and measured spectra, so the chosen equivalent circuit model is correct to describe the thermal behavior of batteries charged at constant current when SOC is between 40% and 60%. Fig. 6 shows the parameters obtained by fitting the spectra to the impedance function in

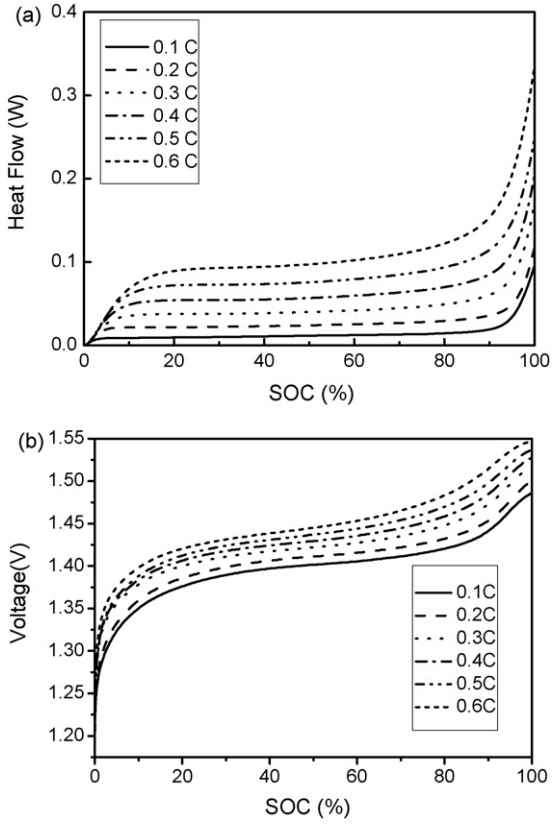

Fig. 4. Heat generation (a) and voltage (b) of sample 1 charged at different rates.

Eq. (15) as function of charge rate. The value of R_t decreases as the charge current increases while the value of C_t increases with the charge current but having a maximum value. The decrease of the value of R_t becomes small which suggests an increase in $\Delta\phi_0$ and ξ_0, so over potential and combination of hydrogen and oxygen increase with charge current. Since C_t has a maximum value, it means $[k_\xi(E_0 + T\Delta S/nF)/I + k_{\Delta\phi}/I]$ has a minimum value when charge current increases. By observing the voltage curves, we find that $k_{\Delta\phi}$ does not change much when charge current grows, so it is the combination of hydrogen and oxygen that grows rapidly after charge rate is higher than 0.5 C. If we want to reduce the electrolyte

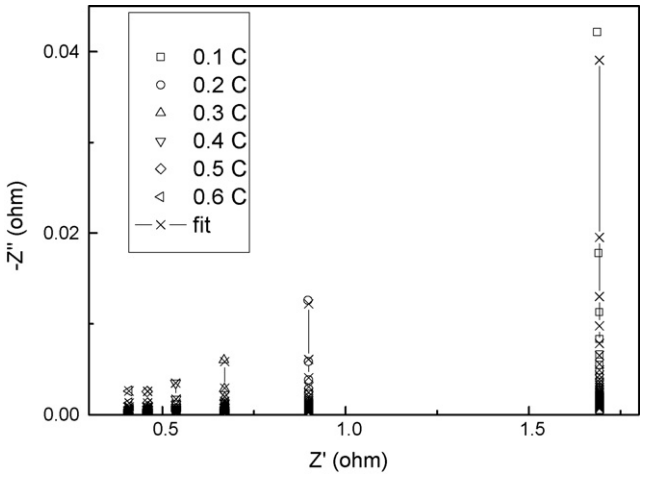

Fig. 5. Impedance spectra of sample 1 charged at different rates. Fit line corresponds to the impedance function for model described by Eq. (15).

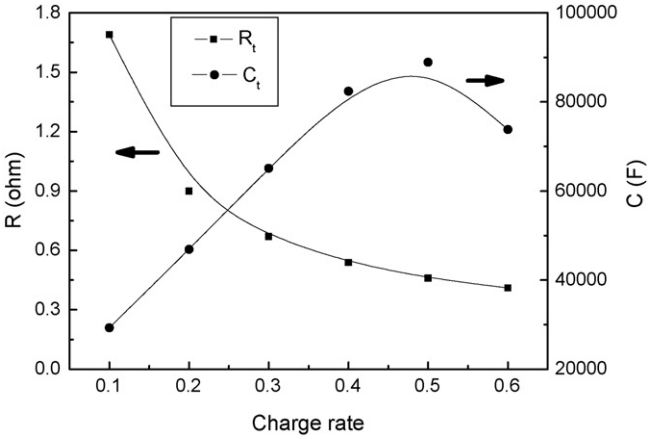

Fig. 6. The values of R_t and C_t resulting from the fit as a function of charge rate.

decomposition of battery, the recommended charge rate is lower than 0.5 C.

4.3. Thermal behavior of Ni-MH battery charged at different temperatures

Fig. 7 shows the heat generation and voltage of sample 1 charged at 0.1 C at 303, 308, 313, 318, and 323 K, respectively. It can be seen that heat generation of battery increases rapidly at the higher temperature, so the charge efficiency decreases due to the increasing evolution of oxygen at the positive electrode [21]. The heat generation before SOC = 15% does not change with temperature, so the reactions at the beginning of charge is independent of tempera-

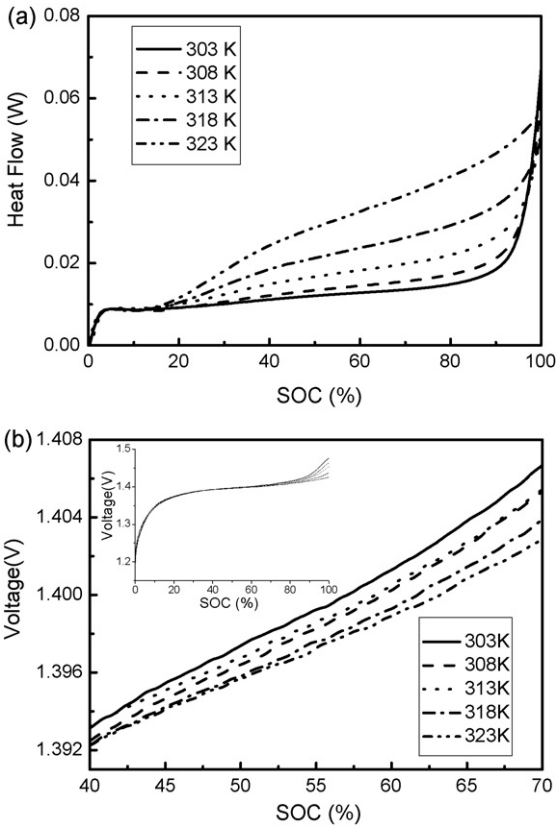

Fig. 7. Heat generation (a) and voltage (b) of sample 1 charged at different constant temperatures.

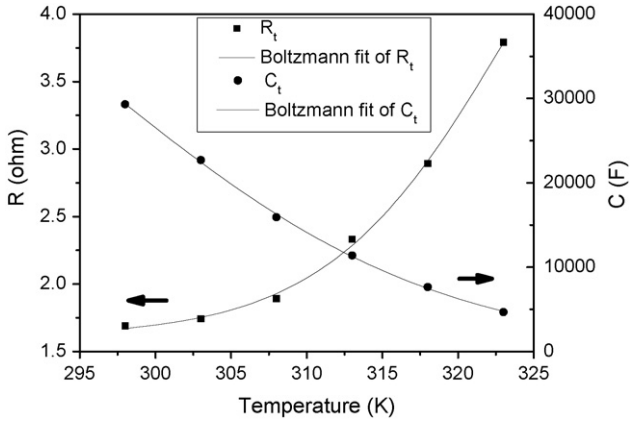

Fig. 8. The values of R_t and C_t resulting from the fit as a function of temperature.

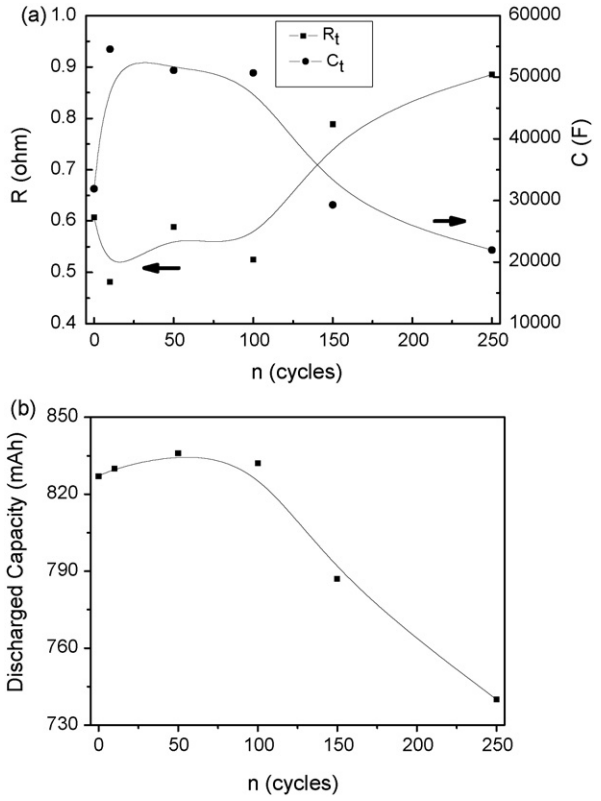

Fig. 9. (a) The values of R_t and C_t resulting from the fit as a function of cycle number, n. (b) Discharged capacity resulting from the fit as a function of cycle number, n.

ture between 303 and 323 K. A plateau can be observed between SOC = 40% and 70% which suggests exothermic reactions becoming slow down in this period. The plateau of heat generation becomes significant as temperature rises which is probably a consequence of the decrease of the over potential as shown in Fig. 7(b). Fig. 8 shows the parameters obtained by fitting the spectra to the impedance function in Eq. (15) as function of temperature. With increasing temperature, the value of R_t increases while the value of C_t decreases. Thus, the charge efficiency decreases and the heat due to combination of hydrogen and oxygen increases as temperature rises. The increase of the value of R_t is slow below 313 K, and battery charged at 298 K has the highest charge efficiency in the temperature range of our experiment. Consequently, if we want the heat generation to be small, the recommended charge temperature is

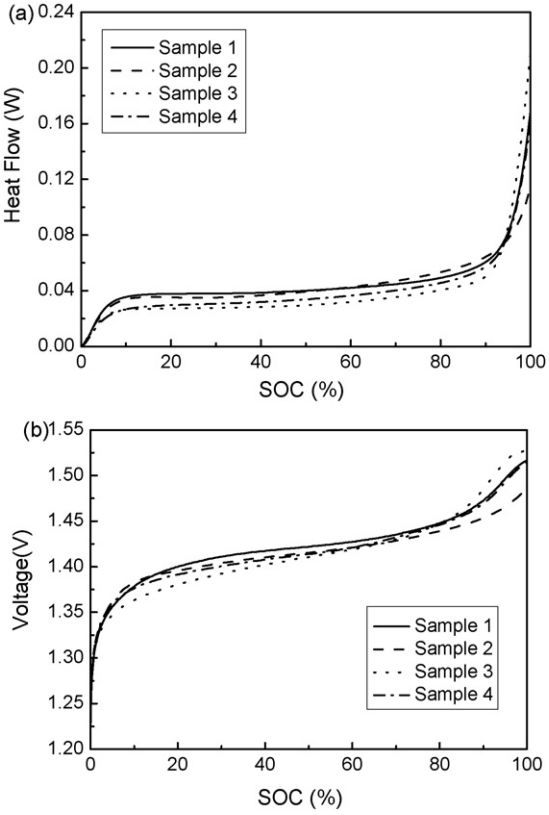

Fig. 10. Heat generation (a) and voltage (b) of batteries from different manufactories charged at same rate.

lower than 313 K. In addition, the two parameters were fitted with a Boltzmann function using origin 7.0 (OriginLab, Inc.) and show good fitting results:

$$y = \frac{A_2 + (A_1 - A_2)}{1 + \exp((x - x_0)/\mathrm{d}x)} \tag{16}$$

The value of C_t is close to 0 when the temperature is 348 K according to the fit. Therefore, battery thermal runaway may happen above 348 K even at low charge rate around half charged. Since heat generation increases with charge rate, we believe that the thermal runaway will happen at lower temperature when charge rate increases.

4.4. Thermal behavior of Ni-MH battery after cycling different times

A high-rate of 2 C was taken to cycle sample 2 at room temperature, and the charge rate was 0.3 C during the test and the temperature was 298 K. The heat generation of sample 2 is obtained at the first cycle, after 10, 50, 100, 150, and 250 cycles, respectively. Fig. 9 shows the relationship of the values of R_t, C_t and discharged capacity with cycle numbers. As shown in Fig. 9(a), it can be seen that the value of R_t is relatively high and the value of C_t is relatively low at the first cycle. In the initial 100 cycles, the value of R_t and C_t show slight change, but the value of R_t increases and the value of C_t decreases rapidly with cycle numbers after 100 cycles. The charge efficiency is low at the first cycle because the active electrode materials are not completely activated, so the discharged capacity grows after several cycles. The battery shows the highest charge efficiency and stable thermal behavior between 10 and 100 cycles, and the heat generation grows significantly after 100 cycles

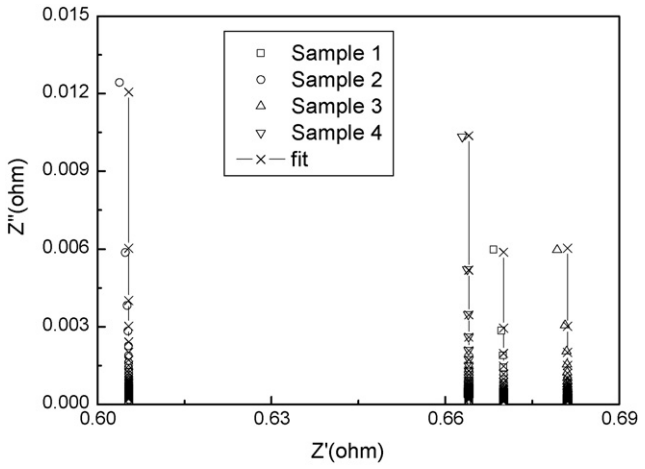

Fig. 11. Impedance spectra of different samples charged at 0.3 C. Fit line corresponds to the impedance function for model described by Eq. (15).

Table 2
The values of R_t and C_t of different samples resulting from the fit

Sample number	R_t (Ω)	C_t (F)
1	0.670	6.48E+04
2	0.605	3.16E+04
3	0.681	6.32E+04
4	0.664	3.68E+04

which results in the decrease of discharged capacity as shown in Fig. 9(b). The results confirm that the internal resistance, which is caused by separator dryout due to swelling of the electrodes, consumption of electrolyte and loss of electrolyte [21], increases with cycle numbers.

4.5. Thermal behavior of Ni-MH batteries from different manufactories with different discharge capacities

Heat-flow for sample batteries from different manufactures with different discharge capacities was measured when they were charged at 298 K. Fig. 10 shows the heat generation and voltage of samples 1–4 charged at 0.3 C, respectively. The heat generation curves of the four samples during charge are very similar and overlapped in time-domain, so we use impedance spectra in frequency-domain to obtain higher resolutions. Impedance spectra of different samples are separated from each other as shown in Fig. 11. The values of R_t and C_t of different samples resulting from the fit are shown in Table 2. By comparing the parameters, we find that samples have different thermal behaviors despite of their same nominal capacity. For example, samples 1 and 2 from two manufactures both have a capacity of 850 mAh, but their values of R_t and C_t are quite different which may be caused by their different designs. However, samples may have similar thermal behaviors although they have different nominal capacities and come from different manufactures. For example, samples 1 and 3 are from different manufactories and with different nominal capacities, but they have similar values of R_t and C_t. In addition, batteries from same manufactures with different capacities may have different thermal behaviors. Samples 2 and 4 are both from GP manufactory but show different values of R_t and C_t which may be caused by different capacities. Therefore, the coherence of thermal behaviors of batteries should better be considered when selecting batteries to assemble battery packs. Batteries with unusual thermal behaviors or generate too much heat during charging or discharging should not be in the battery packs.

5. Conclusions

A novel impedance spectroscopy is obtained in this study. Charge current is used as the excitation signal and heat-flow is used as the response signal to obtain the impedance spectrum. A resistance in series with a capacitance is successfully used as an equivalent circuit to describe the thermal behaviors of batteries during charging when SOC is between 40% and 60%. Heat generation of battery increases with charge rates can be divided into three parts. Impedance spectra in the frequency-domain show that a charge rate higher than 0.5 C may cause rapid heat generation because of the combination of hydrogen and oxygen. Heat generation of battery during charge also increases as temperature increases. The impedance spectra of battery charged at different temperatures show that a recommended temperature for charging is between 298 and 313 K. Thermal runaway may happen when battery is charged at temperature above 348 K even at a low charge rate. The cycling test shows that the charge efficiency of battery is the highest after cycling for 10–100 cycles but decreases after more cycles. Thermal behaviors of batteries from several manufactories with different nominal capacities are compared and samples from the same manufactory have different thermal behaviors may be caused by their different nominal capacities.

The impedance spectrum relates the excitation and response signals, and shows a higher resolution of thermal behaviors of batteries in frequency-domain. If thermocouples are used to instead calorimeter, the testing system can be simplified and be more practical for testing battery packs and large size batteries.

Acknowledgements

The authors appreciate the financial support of the State Key Basic Research Program of China (2002CB211803) and National Natural Science Foundation of China (90410002 and 50606021).

References

[1] T. Araki, M. Nakayama, K. Fukuda, K. Onda, J. Electrochem. Soc. 152 (2005) A1128–A1135.
[2] S. Al Hallaj, J. Prakash, J.R. Selman, J. Power Sources 87 (2000) 186–194.
[3] J.S. Hong, H. Maleki, S. Al Hallaj, L. Redey, J.R. Selman, J. Electrochem. Soc. 145 (1998) 1489–1501.
[4] Z.L. Zhang, M.H. Zhong, F.M. Liu, F.P. Zhong, F. Wu, J. Power Sources 70 (1998) 276–280.
[5] Y. Saito, K. Kanari, K. Takano, T. Masuda, Thermochim. Acta 296 (1997) 75–85.
[6] Y. Saito, K. Kanari, K. Takano, K. Nozaki, J. Power Sources 82 (1999) 913–917.
[7] Y. Saito, K. Takano, K. Kanari, A. Negishi, K. Nozaki, K. Kato, J. Power Sources 97–98 (2001) 688–692.
[8] K. Onda, T. Ohshima, M. Nakayama, K. Fukuda, T. Araki, J. Power Sources 158 (2006) 535–542.
[9] Y. Saito, J. Power Sources 146 (2005) 770–774.
[10] Y. Saito, K. Takano, A. Negishi, J. Power Sources 97–98 (2001) 693–696.
[11] H. Maleki, S. Al Hallaj, J.R. Selman, R.B. Dinwiddie, H. Wang, J. Electrochem. Soc. 146 (1999) 947–954.
[12] R.A. Leising, M.J. Palazzo, E.S. Takeuchi, K.J. Takeuchi, J. Power Sources 97–98 (2001) 681–683.
[13] K. Takano, Y. Saito, K. Kanari, K. Nozaki, K. Kato, A. Negishi, T. Kato, J. Appl. Electrochem. 32 (2002) 251–258.
[14] J.M. Mottard, C. Hannay, E.L. Winandy, J. Power Sources 117 (2003) 212–222.
[15] K. Onda, H. Kameyama, T. Hanamoto, K. Ito, J. Electrochem. Soc. 150 (2003) A285–A291.
[16] J.Z. Shi, F. Wu, S. Chen, C.Z. Zhang, J. Power Sources 157 (2006) 592–599.
[17] E. Barsoukov, S.H. Ryu, H. Lee, J. Electroanal. Chem. 536 (2002) 109–122.
[18] E. Barsoukov, J.H. Jang, H. Lee, J. Power Sources 109 (2002) 313–320.
[19] C.N. Cao, J.Q. Zhang, An Introduction to Electrochemical Impedance Spectroscopy, first ed., Science Press, Beijing, 2002, 1 pp.
[20] X.G. Yang, B.Y. Liaw, J. Electrochem. Soc. 148 (2001) A1023–A1028.
[21] D. Linden, T.B. Reddy, Handbook of Batteries, third ed., McGraw-Hill, New York, 2001, 28.21, 29.24, 30.27 pp.